Since January 2020 Elsevier has created a COVID-19 resource centre with free information in English and Mandarin on the novel coronavirus COVID-19. The COVID-19 resource centre is hosted on Elsevier Connect, the company's public news and information website.

Matter

CellPress

Article

Surfaces with instant and persistent antimicrobial efficacy against bacteria and SARS-CoV-2

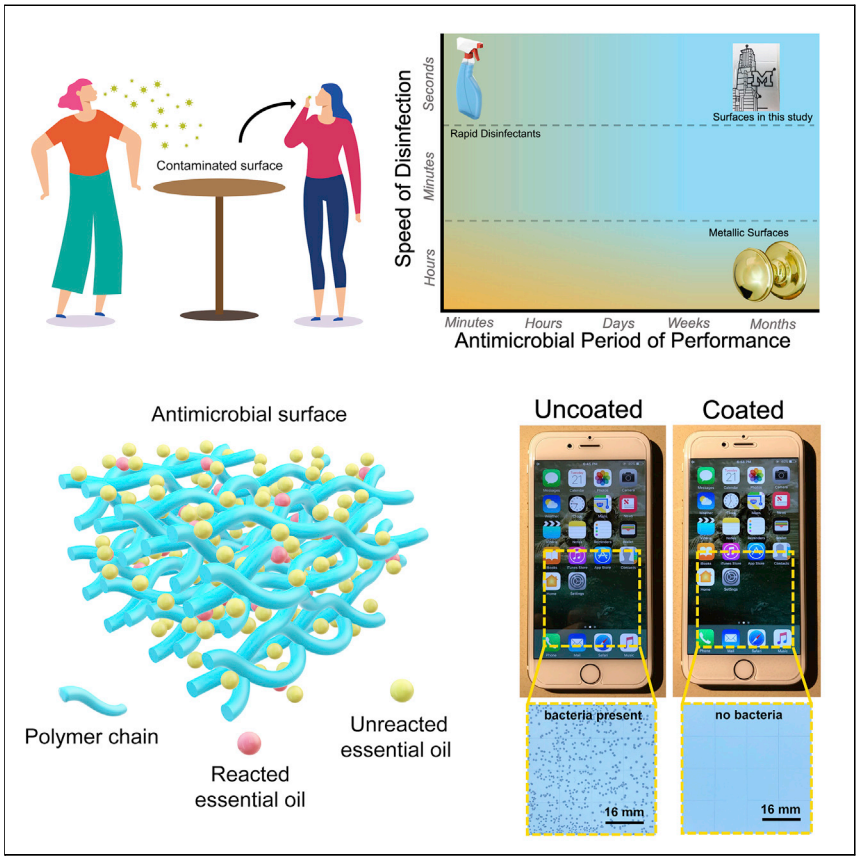

Modern day disinfection either relies on fast-acting, yet impermanent compounds, or slower-acting, long-term antimicrobial surfaces. We have developed a methodology for stabilizing different naturally occurring antimicrobial molecules within a polymer matrix allowing the developed coatings to maintain antimicrobial efficacy for several months. In addition, the developed coatings are durable, easy to apply, and able to inactivate different viruses, and Gram-negative and Gram-positive bacteria, in under 10 min, which is about the same time of action as an antimicrobial wipe.

Improvement
Enhanced performance with innovative design or material control

Abhishek Dhyani, Taylor Repetto, Dylan Bartikofsky, ..., Christiane E. Wobus, J. Scott VanEpps, Anish Tuteja

mehtagee@umich.edu (G.M.)
cwobus@umich.edu (C.E.W.)
jvane@med.umich.edu (J.S.V.)
atuteja@umich.edu (A.T.)

Highlights

Describes durable coatings with instant and persistent antimicrobial activity

Coatings incorporate natural antimicrobial oils that are generally regarded as safe.

Coatings possess broad-spectrum antimicrobial properties

Coatings can be applied to virtually any desired surfaces via dip or spray coating

Dhyani et al., Matter 5, 4076–4091
November 2, 2022
https://doi.org/10.1016/j.matt.2022.08.018

CellPress

Matter

Article

Surfaces with instant and persistent antimicrobial efficacy against bacteria and SARS-CoV-2

Abhishek Dhyani,[1,2,10] Taylor Repetto,[2,3,10] Dylan Bartikofsky,[4] Carmen Mirabelli,[4,9] Zhihe Gao,[1,2] Sarah A. Snyder,[2,3] Catherine Snyder,[2,3] Geeta Mehta,[1,3,7,*] Christiane E. Wobus,[4,*] J. Scott VanEpps,[1,2,6,7,8,*] and Anish Tuteja[1,2,3,5,11,*]

SUMMARY

Surfaces contaminated with bacteria and viruses contribute to the transmission of infectious diseases and pose a significant threat to global public health. Modern day disinfection either relies on fast-acting (>3-log reduction within a few minutes), yet impermanent, liquid-, vapor-, or radiation-based disinfection techniques, or long-lasting, but slower-acting, passive antimicrobial surfaces based on heavy metal surfaces, or metallic nanoparticles. There is currently no surface that provides instant and persistent antimicrobial efficacy against a broad spectrum of bacteria and viruses. In this work, we describe a class of extremely durable antimicrobial surfaces incorporating different plant secondary metabolites that are capable of rapid disinfection (>4-log reduction) of current and emerging pathogens within minutes, while maintaining persistent efficacy over several months and under significant environmental duress. We also show that these surfaces can be readily applied onto a variety of desired substrates or devices via simple application techniques such as spray, flow, or brush coating.

INTRODUCTION

The transmission of bacteria and viruses from surfaces is responsible for the spread of a range of different infectious diseases, hospital-acquired infections (HAIs),[1] contamination of world food supply,[2] as well as threats to homeland security[3] and public health.[4,5] Environmental surfaces in healthcare, public transportation, workplaces, and daycare facilities can provide fomites for pathogen settlement and proliferation over extended periods of time.[6,7] A variety of techniques have been developed thus far to reduce the spread of different pathogens in our environment. Liquid-, vapor-, or radiation-based disinfection techniques are capable of a near-complete elimination of pathogens (>3-log reduction) within a few minutes[8,9] (Figure 1). However, the efficacy of these active surface disinfection methods is short-lived, and surfaces treated with these non-persistent antimicrobial agents can be readily re-contaminated.[10] On the other hand, for more persistent antimicrobial solid surfaces, comprised of heavy metal surfaces, metallic nanoparticles, or surface-tethered biocides, there exists a significant delay between the time of initial contact of the pathogen with the surface and initiation of the pathogen inactivation process (Figure 1). This lag is related to the slow dissolution/transport of the antimicrobial agent across the solid interface, which can take several hours, even for heavy metal ions released from pure metals.[11,12] Therefore, such surfaces may require several hours to complete disinfection (Figure 1),[13–15]

PROGRESS AND POTENTIAL

The transmission of bacteria and viruses from surfaces is responsible for the spread of a range of different infectious diseases, hospital-acquired infections, contamination of world food supply, as well as threats to public health. Modern day disinfection either relies on fast-acting, yet impermanent, liquid-, vapor-, or radiation-based disinfection techniques, or slower-acting, passive antimicrobial surfaces based on somewhat toxic heavy metals or surface-tethered biocides. This divide between rapid disinfection and long-lived antimicrobial efficacy is an inherent problem in modern day disinfection due to the prompt evaporation from the surface of agents capable of rapid disinfection, and the slow dissolution/diffusion of heavy metal ions or tethered biocides. Here, we describe a class of solid surfaces with instant antimicrobial efficacy (>4-log reduction within a few minutes) against a wide spectrum of pathogenic species, including SARS-CoV-2, while retaining their antimicrobial efficacy even after several months of environmental exposure, repeated contamination cycles, and extreme mechanical, chemical, and thermal duress.

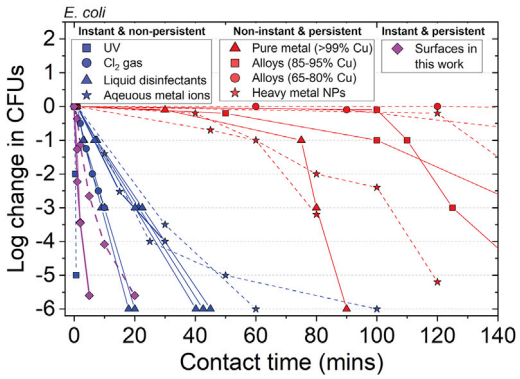

Figure 1. Dichotomy of instant and persistent antimicrobial technologies

Escherichia coli kill rates using instant and non-persistent disinfection methods including UV,[17] Cl_2 gas,[18] liquid disinfectants,[9] and aqueous Ag+ ions.[19–21] In this study, comparison is made with non-instant but more persistent antimicrobial solid surfaces comprising pure copper, its alloys,[2,13] heavy metal-based nanoparticles,[15,22] and surfaces. Error bars for literature data were not extractable from literature sources.

thereby increasing the chances of pathogen transmission from highly touched surfaces. In addition, heavy metal-based antimicrobial surfaces also suffer from various toxicity concerns.[16] In this work, we have developed a class of solid surfaces with instant antimicrobial efficacy (>4-log reduction within a few minutes of contact) against a wide spectrum of current and emerging pathogenic species, while maintaining persistence of their antimicrobial performance over several months and under extreme mechanical, chemical, and thermal duress.

Over centuries, plants have evolved remarkable survival strategies against a plethora of continuously evolving viruses, bacteria, fungi, and insects.[23] One strategy involves surface secretions of plant secondary metabolites, specifically essential oils, through outgrowths called glandular trichomes spread on a plant's surface.[24] These secondary metabolites provide broad-spectrum surface and airborne protection against different pathogenic threats through a variety of mechanisms including causing cell membrane disintegration and binding to proteins to inactive them.[25–28] Even today, plants continue to modify their internal chemistries and metabolite compositions to meet evolutionary demands.[23] The extreme volatility of essential oils, however, makes them unsuitable for persistent antimicrobial efficacy (Figure S1). Moreover, Figure S2 and Table S1 show that their composition, and thereby antimicrobial efficacy, can change with geographic origin, production lots, and environmental aging. The choice of a single component, as opposed to a natural oil, which is a mixture of different compounds, ensures reproducible and consistent antimicrobial efficacy. For this study, we selected α-terpineol or *p*-menth-1-en-8-ol (AT), a terpenoid present in the essential oil of *Melaleuca alternifolia* (tea tree oil [TTO]) as the antimicrobial agent of choice. AT was chosen because it has been shown to be an active antimicrobial against a broad spectrum of pathogens and is already approved by the FDA and European Commission as a food additive for human consumption.[29–32] Furthermore, AT has a larger half-maximal inhibitory concentration against human foreskin fibroblasts than commercial antiseptics already approved for direct skin contact for disinfection (also see Table S2).

RESULTS AND DISCUSSION

Stabilization of the antimicrobial agents

In the past, polymer carriers and their conjugates have been used for prolonging the lifespans of different small and large functional molecules, such as proteins,

[1]Macromolecular Science and Engineering, University of Michigan, Ann Arbor, MI 48109, USA

[2]Biointerfaces Institute, University of Michigan, Ann Arbor, MI 48109, USA

[3]Department of Materials Science and Engineering, University of Michigan, Ann Arbor, MI 48109, USA

[4]Department of Microbiology and Immunology, University of Michigan, Ann Arbor, MI 48109, USA

[5]Department of Chemical Engineering, University of Michigan, Ann Arbor, MI 48109, USA

[6]Departments of Emergency Medicine, University of Michigan, Ann Arbor, MI 48109, USA

[7]Department of Biomedical Engineering, University of Michigan, Ann Arbor, MI 48109, USA

[8]Michigan Center for Integrative Research in Critical Care, University of Michigan, Ann Arbor, MI 48109, USA

[9]Present address: Institute of Virology and Cell Biology, University of Lübeck, Lübeck 23562, Germany

[10]These authors contributed equally

[11]Lead contact

*Correspondence: mehtagee@umich.edu (G.M.), cwobus@umich.edu (C.E.W.), jvane@med.umich.edu (J.S.V.), atuteja@umich.edu (A.T.)

https://doi.org/10.1016/j.matt.2022.08.018

antibodies, and drugs against environmental stressors, and for controlling their release profiles into their respective environment.[33,34] We utilized a similar strategy to stabilize AT within a polymer, while maintaining its antimicrobial efficacy.

We first allowed a fraction of the hydroxyl bearing AT to covalently react with an isocyanate (Desmodur N3800; Covestro) to yield a partially conjugated isocyanate (Figure S3). The remaining unreacted isocyanate groups were then crosslinked with a polyol (Desmophen 670BA; Covestro). This yields a solid polyurethane (PU) with a fraction of AT that is covalently bound within the elastomer as elucidated by Fourier transform infrared spectroscopy (Figure S4). This covalently bound fraction stabilizes and controls the release of the remaining unreacted AT, which was quantified using thermogravimetric analysis as shown in Figure S5. Similarly, essential oils such as TTO, that contain several different antimicrobial components including hydroxyl-bearing terpenoids, can also be stabilized within a PU network (Figure S6).

Controlling disinfection speeds for Gram-negative and Gram-positive bacteria

The rate of disinfection on a surface increases with increasing concentration of the antimicrobial agent on the surface. This has been observed for various solid antimicrobial surfaces, including copper and its alloys.[13,14] To tune the surface concentration of the natural oil-based antimicrobials on the PU surface, we vary the concentration of the antimicrobial agent added before crosslinking. Typically, the surface fraction of an oil for an oil-filled polymer system is not the same as the fraction of oil added to the bulk.[35] This is because, in a binary mixture, the low-surface energy component, either the oil or the polymer, preferentially migrates to the air interface to lower the overall surface free energy.[35,36]

Consider ϕ_s and $1 - \phi_s$ to be the surface fractions of the polymer and oil phases, respectively, for an oil-filled polymer. The apparent contact angle, θ^*, for a liquid droplet on the surface of a solid filled with the same liquid, can be found by applying the Cassie-Baxter equation[37,38] as, $\cos\Theta^* = (1 - \phi_s)\cos 0^\circ + \phi_s \cos\Theta_E$. Here, Θ_E is the equilibrium contact angle of the liquid over the (unfilled) solid. Thus, by simply measuring the apparent and equilibrium contact angles, one can determine the surface fractions of the oil and polymer phases.

For PU+AT surfaces, we observed a partially wetted, non-lubricated surface (i.e., $\theta^* > 0^\circ$ and $\phi_s > 0$) at AT concentrations $\leq 70\%$ (weight %), whereas at 80%AT, a lubricated surface was created ($\phi_s = 0$). Figure S7 also shows the systematic variation in the surface fraction of AT, with the amount of AT added before urethane crosslinking. Overall, by controlling the amounts of total and reacted fractions of the antimicrobial agent, we can tune the surface fraction of the antimicrobial agent and its release from the polymer.

To evaluate the disinfection kinetics on the fabricated antimicrobial surfaces, we used *Escherichia coli* as a model Gram-negative bacterium. *E. coli* is a well-known pathogen responsible for urinary tract infections, as well as foodborne illnesses.[2,39] With many current disinfection technologies, the log survivor-time curves for *E. coli* for dilute chemical disinfectant solutions and aqueous heavy metal ions follow a concave downward trend[8,40,41] (Figure 1). This behavior is observed when (1) disinfection kinetics are not rate limited by the diffusion of the antimicrobial agent and (2) the biocide is not in excess relative to the pathogen concentration.[8,40,41] When the antimicrobial agent is in excess relative to the pathogen concentration, the log survivor-time curve is generally linear[41] as seen during rapid disinfection via UV and chlorine gas[17,18] (Figure 1). In contrast, this correlation is concave upward for most

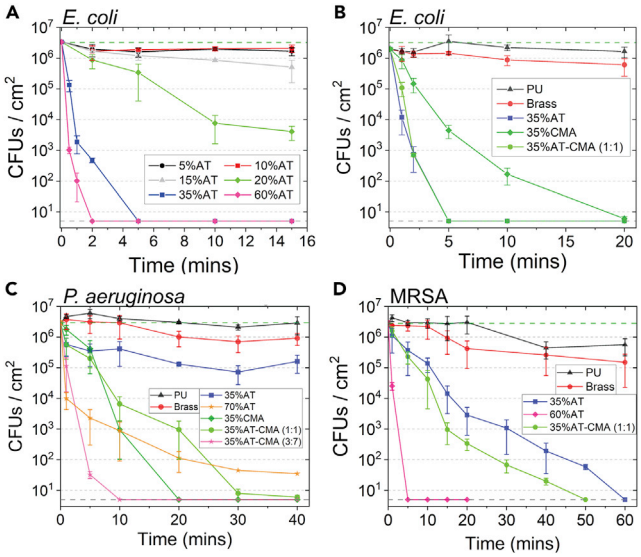

Figure 2. Controlling the speed of disinfection against Gram-negative and Gram-positive bacteria

(A) Survival of an initial inoculum (green dashed line) of ~3 × 10^6 CFU/cm^2 of *E. coli* (UTI89) on surfaces with different fractions of AT, plotted against time, at room temperature (similar to ISO 22196). PU+60%AT showed a rapid ~3.5-log and ~5.8-log reduction in CFUs of *E. coli* in 30 s and 2 min, respectively. Gray dashed line at 5 CFUs/cm^2 represents limit of detection.

(B–D) Survival of (B) *E. coli*, (C) *P. aeruginosa*, and (D) MRSA on surfaces with AT, CMA, and their combinations. Similar to *E. coli*, larger fractions of AT were effective against *P. aeruginosa* and MRSA as well. PU+35%AT-CMA (3:7) displayed a faster kill rate against *P. aeruginosa* compared with PU+35%AT and PU+35%CMA, indicating synergistic action. Error bars represent 1 SD; N = 3 independent experiments with triplicate measures.

metallic or other solid biocidal surfaces due to the temporal lag between the initial pathogen-biocide contact and the onset of the pathogen inactivation process during which the metal ions/biocide diffuses across the solid interface[42] (Figure 1).

To evaluate the antimicrobial performance of the fabricated surfaces, we mimicked a severe surface contamination event by spreading a 10 μL droplet containing a suspension of ~3 × 10^6 *E. coli* over a 1 cm^2 area on the surface of the sample. This test is similar to the ISO 22196 standard method utilized for evaluating the antimicrobial performance of different non-porous solids. At specific time intervals, the bacteria were recovered in PBS and the dispersed bacterial cells were enumerated using serial dilutions and agar plating. Since this test measures the number of bacterial cells present on a surface, a simple low-adhesion surface without an active antimicrobial agent would show microbial contamination.

We systematically varied the fraction of AT stabilized within PU and confirmed that the surface disinfection rate directly correlated with the weight fraction (and therefore, the surface fraction) of AT (Figure 2A). As the fraction of AT was increased from 5% to 35%, the log survivor-time curves displayed a concave downward trend (Figure 2A), i.e., the diffusion of AT at the solid interface was not found to be rate limiting. By further increasing the bulk AT fraction to 60%, we were able to reduce the time required to achieve a >3-log reduction (>99.9% kill) in the number of viable bacteria, from several minutes to a few seconds. For this surface, the log survivor-time curve is approximately linear, indicating that the surface fraction of AT was in excess relative to the concentration of *E. coli*. The surfaces displayed a ~5.8-log

reduction for *E. coli* in under 2 min. These kill times are much faster than the treating time recommended for common chemical disinfectants,[9] heavy metal surfaces,[2,13] nanoparticles,[15,22] and their salt solutions[19,20] (Figures 1 and 2B). These results were further confirmed using fluorescence microscopy (Figure S8; Video S1). These observations highlight that the coating's pathogen kill rate can be tailored to not only overcome diffusion rate-limited disinfection kinetics but to even attain disinfection times faster than current active disinfection methods (Figure 1).

To challenge these surfaces with a pathogen known to have a higher resistance to AT, we tested their performance against another Gram-negative bacterium, *Psuedomonas aeruginosa*, a frequent cause of nosocomial infections.[43] As expected, due to the relatively high minimum inhibitory concentration (MIC) of AT against *P. aeruginosa* compared with *E. coli* (Table S3), higher weight fractions of AT were required for achieving disinfection (Figure 2C). Although incorporating a higher loading of the antimicrobial agent within the polymer is an effective strategy, choosing an agent with a lower MIC would, by definition, lead to a higher antimicrobial activity per unit volume. We identified cinnamaldehyde (CMA), a component of the essential oil from the genus Cinnamomum, to be an effective antimicrobial agent against *P. aeruginosa* (Table S3). CMA has a higher antimicrobial potency against *P. aeruginosa* compared with AT. This is likely because of the different mechanisms of pathogen inactivation for CMA versus AT.[25] While maintaining a 35% oil fraction in PU, we optimized the ratio of AT and CMA to display a 4.9-log reduction in *P. aeruginosa* in under 5 min. We observed that a 3:7 AT:CMA ratio blend displayed synergistic effects and faster kill rates than PU with CMA or AT alone at the same oil fraction (35%) (Figure 2C). The ability to incorporate different antimicrobial agents, either individually or in combination, offers significant advantages in selectively targeting specific pathogenic species for a given application environment. This ability also reduces the likelihood of the pathogens developing drug resistance,[44] as different antimicrobial agents with distinct mechanisms of action for killing pathogens can be selected.

To investigate the broad-spectrum antimicrobial efficacy of the developed surfaces, we evaluated their efficacy against a representative Gram-positive pathogen, methicillin-resistant *Staphylococcus aureus* (MRSA). MRSA is commonly found in hospitals and nursing homes, and is a major contributor to HAIs around the globe.[1] Increasing the fraction of AT from 35% to 60%, we observed a transition in the log survivor-time curve from concave downward to linear, indicating that the AT surface fraction was in excess of the concentration of MRSA cells.[41] For 60%AT, we measured a ~5.8-log reduction in MRSA over a time period of 5 min (Figure 2D). These inactivation times are orders of magnitude lower than those for the current state-of-the-art copper-containing materials, which can take several hours to achieve similar levels of disinfection against MRSA and *P. aeruginosa*.[45]

Achieving persistent antimicrobial efficacy

Surfaces disinfected with current active disinfection techniques are vulnerable to re-contamination from successive pathogenic attacks.[5,46] Therefore, we tested the performance of PU+35%AT over multiple contamination cycles by contacting the surface with ~10^6 cells of *E. coli* every 30 min and determined the bacterial counts after each exposure. PU+35%AT was chosen for the persistency tests due to its superior mechanical durability under ASTM D4060 compared with higher AT concentrations. The surface repeatedly displayed a ~5.3-log reduction (>99.9995% kill) after every contamination cycle for up to eight cycles (Figure 3A) highlighting its persistent antimicrobial efficacy.

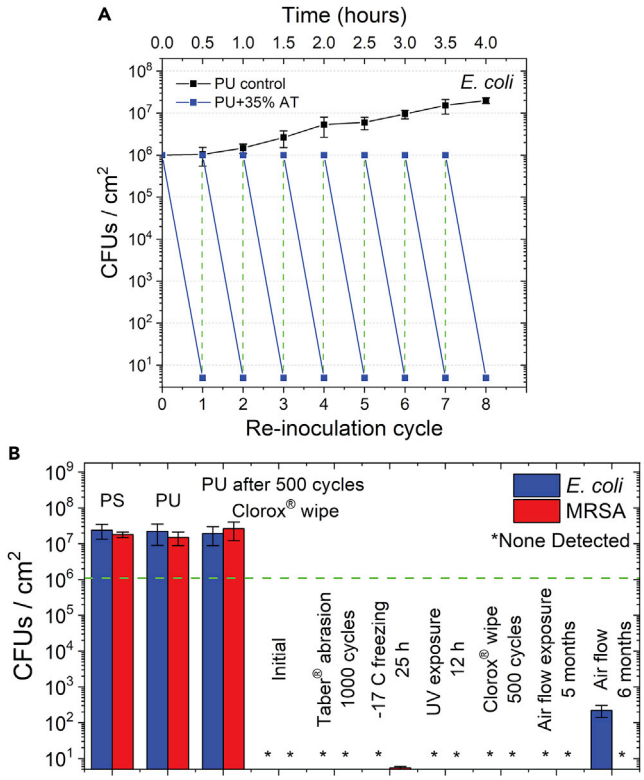

Figure 3. Persistent antimicrobial efficacy

(A) Eight successive *E. coli* contamination cycles highlighting the continuous, rapid bactericidal properties of PU+35%AT. In each cycle, the surfaces were contacted with ~10^6 cells/cm^2.

(B) Total CFUs/cm^2 of *E. coli* and MRSA recovered from control (PU and PS) and test surfaces after 24 h at 37°C from an initial broth inoculum of ~10^6 cells/mL (green line). No CFUs were detected for PU+35% AT (limit of detection = 5 CFUs/cm^2) showing a ~5.3-log reduction. The graph also shows persistent antimicrobial performance of PU+35%AT after exposure to extreme conditions of mechanical and chemical (Clorox) abrasion, UV exposure, freezing conditions, and accelerated aging under air flow for up to 5 months. After 6 months, the surface's efficacy is maintained against MRSA but reduced against *E. coli*. Error bars represent 1 SD; N = 3 independent experiments with triplicate measures.

Antimicrobial surfaces that are utilized in real-world operating environments need to display significant durability over long periods of time.[46] We next evaluated the persistent antimicrobial efficacy of the fabricated coatings under mechanical, chemical, and thermal duress. We subjected the fabricated antimicrobial coatings to a series of simulated environmental tests (see experimental procedures), before contacting them with a high bacterial load under dynamic contact conditions. Accelerated weathering conditions were mimicked via continuous exposure to air flow for up to 6 months (Figure 3B). We consistently observed a 5.3-log reduction in bacterial loads against *E. coli* and MRSA during this period. After the sixth month of continuous air exposure, the coating displayed a 3.7-log reduction against *E. coli* but maintained a 5.3-log reduction against MRSA. The likely reason for this is that MRSA is a Gram-positive bacteria and *E. coli* is a Gram-negative bacteria. Essential oils generally show greater antimicrobial efficacy against Gram-positive bacteria because they lack an outer membrane that protects cells against hydrophobic molecules. The loss in performance against *E. coli* is likely a result of loss in the bulk AT content within the polymer (Figure S9). In addition, 1,000 cycles of CS-10 Taber abrasion (under 0.8 kg load; ASTM D4060), 500 cycles of chemical cleaning with Clorox wipes (under 1.1 kg

load), 12 h of UV exposure, and 25 h exposure to freezing environment (−17°C) were also performed on the coatings. After each test, sections were tested against MRSA and *E. coli* via broth culture (see experimental procedures). We continued to observe a 5.3-log reduction in viable bacterial cells. As a control, we tested PU that was similarly cleaned with Clorox wipes, rinsed and dried for 30 min before contacting with bacteria, and observed a 1.4-log and 1.3-log increase for MRSA and *E. coli*, respectively, after 24 h of incubation (Figure 3B). These data demonstrate the coating's persistent antimicrobial performance, which outperforms even heavy metal-containing ceramics.[45]

Instant and persistent inactivation efficacy against SARS-CoV-2

As stated earlier, fomites can play a significant role in the transmission of bacteria and viruses.[1,42,47] Viruses in particular can remain viable on surfaces for long periods of time. As an example, the stability of the current human coronavirus SARS-CoV-2 on different surfaces for multiple days is in part fueling the ongoing COVID-19 pandemic[42,47] (Figure 4A). Thus, we evaluated the stability of SARS-CoV-2 as a model virus on two experimental surfaces, PU+35%AT and PU+70%AT. The base PU without AT and aluminum served as controls (see experimental procedures). For the PU+35%AT, a 4.0-log reduction was observed after 60 min of contact (Figure 4B). For PU+70%AT, we observed an instant 1.6-log reduction after 10 min, and a 4.3-log reduction (>99.99%) after 30 min of contact (Figure 4B). The data illustrate a concentration dependence on the speed of virus inactivation on the surface. In addition, the nearly linear log survivor-time curve suggests close to excess concentrations of the antimicrobial agent relative to the virus. Finally, current active disinfection techniques are short-lived, and most persistent disinfecting surfaces display a low viral inactivation rate.[48,49] In contrast, we show that the fast-acting antimicrobial surfaces fabricated here can maintain their virucidal capabilities even after 2 weeks (Figure 4B).

Applications of instant and persistent antimicrobial surfaces

We next demonstrated the ease of application using common commercial coating methods (dip, spray, or brush coating), as well as the utility of the developed coatings in different settings. The coating methodologies used here do not require specialized equipment that is not already utilized in the field, which may allow for an easier transition from the laboratory to commercial utilization. Studies have shown the significant prevalence of bacterial and viral contamination on different hospital surfaces including keyboards, doorknobs, bed rails, and phones.[1] Pathogens, such as MRSA, are particularly at fault for causing nosocomial infections. To mimic the contamination of a keyboard during use, we typed a pangram with gloves contaminated with MRSA over an uncoated keyboard, and a keyboard spray coated with PU+35%AT (thickness = 37 $\pm$ 2 μm; see experimental procedures). The coating is transparent (Figure S10), flexible, and maintained the keyboard's mechanical, electronic functions. Ten minutes after microbial contact, we recovered >6,000 CFUs from the swabs of the uncoated keyboard, while the keyboard coated with PU+35%AT displayed only 5 CFUs (Figure 5A).

Food contact surfaces can possess extremely high bacterial loads of $\sim 10^5$–10^9 CFU/cm^2, along with the associated risk of causing large-scale foodborne illness outbreaks.[1,2,18] We brush coated half of a polypropylene cutting board with a biomedical-grade PU (Baymedix, Covestro), BM, incorporated with AT (BM+35%AT) and left the other half uncoated. For the cutting board and gauze, BM was chosen as it is a medical-grade PU that meets medical device standards. To mimic contamination

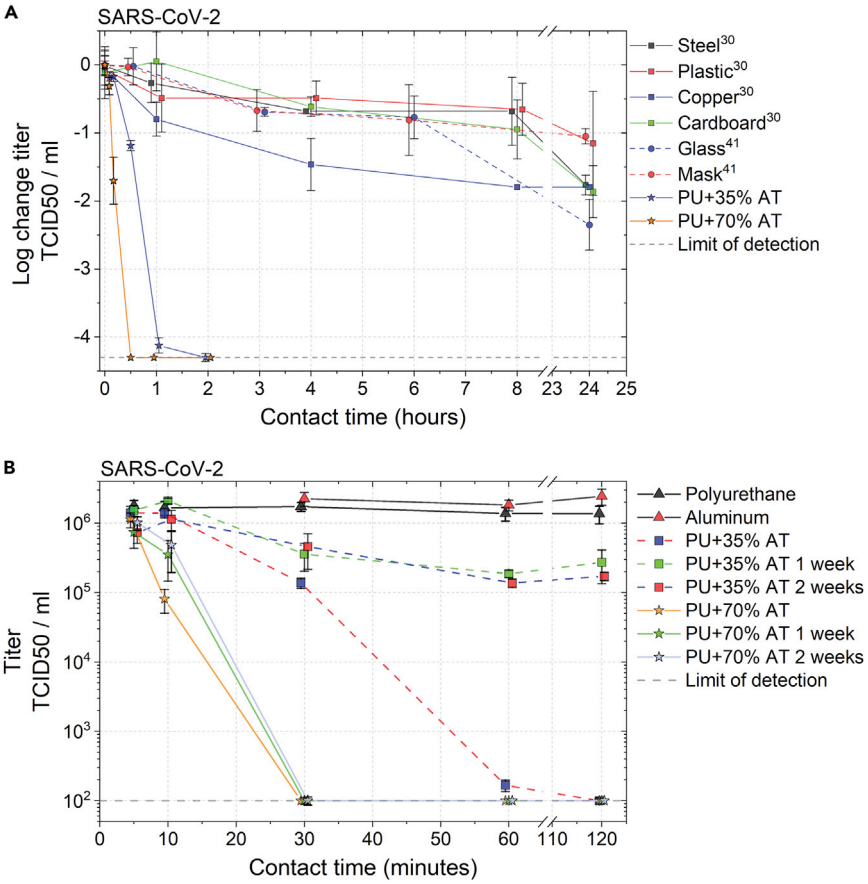

Figure 4. Survival and inactivation of SARS-CoV-2 on different surfaces

(A) Comparison of SARS-CoV-2 inactivation on different surfaces in the literature[42,47] and this work. Error bars represent SD; N = 2–3 independent experiments with three technical replicates each.

(B) Infectivity of SARS-CoV-2 (starting viral load of 2.5 × 10^7 TCID50/mL) on PU+35%AT and PU+70%AT surfaces plotted against the contact time of the virus with the surface. The speed of inactivation of the virus on the surface increases with the fraction of AT. Within just 10 and 30 min, a 1.7-log and 4.3-log reduction, respectively, was observed for PU+70%AT. The PU+70%AT surface maintained its 4.3-log reduction in 30 min even after environmental exposure for 1- and 2-week periods without any external disinfection. Error bars represent 1 SE of mean; N = 2–3 independent experiments with three technical replicates each. The gray dashed line represents the limit of detection of the TCID50 assay (2 Log10 TCID50/mL).

from food, both halves were then contacted with thawed chicken flesh for 20 min at room temperature (see experimental procedures and Figure 5B). The flesh was removed, and the surfaces were left to sit for 20 min in ambient air before swabbing the surfaces for bacteria. The uncoated side showed heavy microbial contamination (4 × 10^6 CFU) from the swab, while the coated side only showed 15 CFUs, a 5.4-log (>99.999%) reduction.

The surfaces of mobile phones and other touch devices can also spread communal infections.[1] In addition, these surfaces are required to be transparent and touch sensitive. Therefore, we next coated a glass cell phone screen protector with PU+35% AT that did not affect its touchscreen functionality (see Video S2) and optical transparency (see Figure S10). Gloved thumbs contaminated with ~1.6 × 10^5 *E. coli* cells were applied in a specific pattern covering the whole screen of the coated screen protector, along with an unmodified hydrophobic control (see experimental

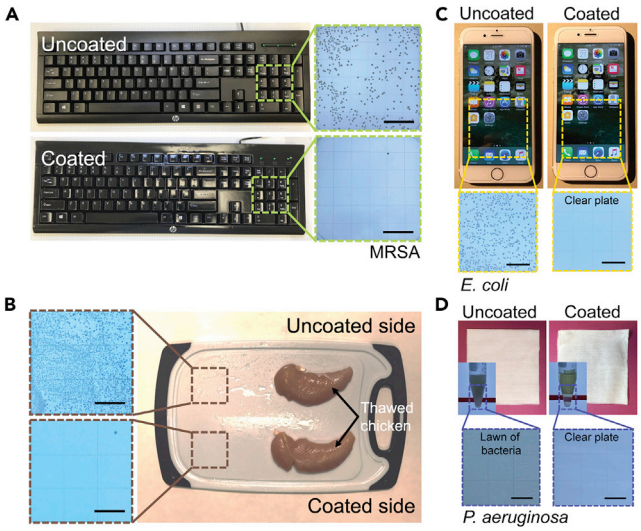

Figure 5. Applications of the fabricated surfaces

(A) Uncoated and spray-coated keyboards with PU+35%AT are contacted with gloved fingers contaminated with MRSA. Ten minutes post contamination, bacterial colonies on the keyboard were enumerated. The coated keyboard showed a 3.1-log or 99.9% reduction with respect to the uncoated keyboard. Scale bar, 23 mm. The spray-coated keyboard retained its electronic function.

(B) A cutting board, half brush coated with BM+35%AT, was contacted with thawed chicken. Scale bar, 12 mm. Approximately 4×10^6 CFU were recovered from the swabs for the uncoated side of the board, while the coated side showed only 15 CFUs, a 5.4-log reduction after 20 min.

(C) Cell phones with an uncoated and a PU+35%AT-coated screen protector. Gloved thumbs with ~1.5×10^5 *E. coli* cells were contacted in a specific pattern (Figure S14) over the phones. After 2 min, the uncoated screen showed a total of ~6,000 CFUs while no CFUs were detected on the coated surface. Scale bar, 16 mm.

(D) Uncoated and coated medical gauze with BM+60%AT-CMA (3:7). The inset shows 2 cm^2 pieces of the respective gauze after 24 h of incubation (37°C) in a broth culture containing *P. aeruginosa*. The coated gauze displayed an ~8.2-log reduction compared with the uncoated dressing. Scale bar, 11 mm. All images of colonies represent a 5-fold dilution of the recovery solution.

procedures and Figure S14). Both surfaces were swabbed initially and after 2 min to enumerate the bacterial load. About 6,000 CFUs were transferred on both phone screen surfaces. The uncoated phone screen did not show any signs of bacterial reduction, while complete elimination of live bacteria was observed on the coated phone screen after 2 min (Figure 5C). The applied coating on these substrates was much thinner (30–200 μm) than the coatings tested previously (1 mm), highlighting that the speed of disinfection is likely not impacted by coating thickness. In addition, the coatings applied to the keyboard, cutting board, and cell phone screen protector remained adhered for at least a year.

We also applied BM+60%AT-CMA (3:7) on a porous medical gauze (Figures 5D and S13) and immersed a section of the gauze in a broth culture containing ~10^6 cells of *P. aeruginosa* (see experimental procedures). After 24 h of incubation at 37°C, we observed no bacterial growth in the dressing for the coated gauze compared with an 8.2-log reduction of an uncoated dressing. These findings could be extremely useful for reducing the colonization of infectious pathogens within wound dressings or other porous substrates, such as face masks. In addition, we report a primary skin irritation index of 0.0 for BM+60%AT verified by ISO 10993-10 test (see experimental procedures). These results illustrate that the fabricated coatings possess no significant quantity of biologically harmful extractables—a finding that is crucial for medical devices and skin-contact applications.

Table 1. MICs of AT after 10 cultivation steps

Generation no.		1	2	3	4	5	6	7	8	9	10
MIC (v/v, %)	run 1	0.20	0.25	0.25	0.25	0.25	0.25	0.25	0.25	0.25	0.25
	run 2	0.20	0.20	0.20	0.20	0.20	0.20	0.20	0.20	0.20	0.20
	run 3	0.20	0.20	0.20	0.20	0.20	0.25	0.20	0.20	0.25	0.20

MIC of AT as determined for Gram-negative *E. coli* after each of the 10 consequent cultivation steps.

Reducing the likelihood of drug resistance

The evolutionary trait of bacterial and viral drug resistance has contributed to communal epidemics in the past.[50] Specifically, for a commensal bacterium like *E. coli*, the increasing prevalence of its antibiotic-resistant variants has exacerbated efforts to counteract urinary tract infections and foodborne diseases in diverse communities.[2,18] In addition, multiple reports have now shown increasing resistance and cross-resistance to silver, copper, and other metal ions by different bacteria, including *E. coli*.[51,52] To determine the likelihood of generating a resistant strain of *E. coli* against AT, we performed 10 successive bacterial cultivation steps in agar containing sub-inhibitory AT concentrations (0.1–0.5, v/v, %) and determined the MICs of the AT after each cultivation as described in Wiegand et al.[53] (Table 1). No appreciable increase in AT MIC was observed for *E. coli* for up to 10 generations. These observations are also in agreement with Hammer et al. who found no significant change in antimicrobial susceptibility of *E. coli* to tea tree oil and its components.[54] Overall, these results, along with the known distinct mechanisms of antimicrobial action of different essential oil components,[25] may provide a pathway for designer antimicrobial surfaces incorporating different blended antimicrobial agents that reduce the likelihood of inducing antimicrobial resistance.[44]

Limitations of the study

One limitation of the current study is that the antimicrobial efficacy was only tested on surfaces aged up to 6 months. Thus, the time point at which the surfaces will cease to be antimicrobial is unknown. In addition, while the surfaces are effective against an enveloped virus, SARS-CoV-2, the antiviral efficacy of the surfaces against non-enveloped viruses, such as norovirus, has not yet been evaluated.

Conclusion

In summary, this work demonstrates a unique approach for fabricating broad-spectrum antimicrobial surfaces by utilizing natural, low-toxicity, antimicrobial molecules, and blends. The efficacy of these surfaces can be tailored via antimicrobial agent concentration and synergistic combinations enabling inactivation time frames of a few minutes against a variety of Gram-negative and Gram-positive bacteria and SARS-CoV-2. These disinfection time frames are currently only provided by active disinfection methods, which are impermanent. We show that these surfaces can maintain their antimicrobial efficacy over several months of air exposure and after significant mechanical, chemical, and thermal duress. This approach also enables the fabrication of designer antimicrobial surfaces that can facilitate protection from specific microbes and limit the likelihood of developing antimicrobial-resistant pathogens against current and future pathogenic threats to society.

EXPERIMENTAL PROCEDURES

Resource availability

Lead contact

Further information and requests for resources and reagents should be directed to and will be fulfilled by the lead contact, Anish Tuteja (atuteja@umich.edu).

Materials availability

This study did not generate new unique reagents.

Data and code availability

Any additional information required to reanalyze the data reported in this paper is available from the lead contact upon request.

Surface fabrication

PU surfaces were fabricated by reacting 46.36 wt % of the isocyanate, Desmodur N3800 (Covestro) with 53.63 wt % of the polyol, Desmophen 670 BA (Covestro). The mixture is mixed homogenously, degassed if needed, drop cast on glass slides, and cured at room temperature for 4–6 days; 0.1 wt % dibutyltin dilaurate (DBTL) (Sigma Aldrich, product code 291234) or bismuth neodecanoate (Gelest; product code CXBI061) may be used as catalyst to speed up curing to 24–36 h (solid to touch) at room temperature. To fabricate PU surfaces with AT (Sigma Aldrich, product code W304522) or TTO, Desmodur N3800, the antimicrobial agent and 0.1 wt % DBTL were mixed and allowed to react for a specific time depending on the reacted content required (Figure S3). Specifically, to fabricate PU+35%AT, Desmodur N3800 was allowed to react with 35 wt % AT in the presence of 0.1 wt % DBTL catalyst for 3 h. Then, Desmophen 670 BA was added to the isocyanate-AT-catalyst mixture and mixed. The mixture is drop cast on glass slides and cured at room temperature for at least 24 h (96 h in the absence of a catalyst) inside a covered Petri dish to avoid evaporation of the agent. Note, the coating is solidified within 24 h, but longer times are needed to achieve full cure. The thickness of the coating can be varied from 50 μm to 1 mm by using acetone or methyl isobutyl ketone as the solvent. Since the speed of disinfection depends on the surface fraction of the agent, the coating thickness only controls the antimicrobial agent reservoir volume for persistent efficacy. Surfaces with 0 wt % reacted fractions were fabricated by swelling the PU control in ethanol, and drying and swelling it in the agent. For spray and brush coating applications, acetone was used as solvent. Similarly, medical-grade PU precursors, 10.85 wt % of Baymedix AP501 (isocyanate; Covestro) and 54.15 wt % of Baymedix AR602 (polyol; Covestro) along with 35 wt %AT were used to fabricate BM+35%AT. 0.3 wt % bismuth neodecanoate was used as the catalyst for the Baymedix PUs.

Durability and environmental stability

To observe the effects of environmental aging on PU+35%AT, the coating was kept inside a fume hood under continuous air flow at 100 feet per minute and tested for bacterial growth as well as the oil weight fraction periodically for up to 6 months. Mechanical abrasion was performed using a Linear Taber Abrasion machine with a CS-10 resilient abrader and a total weight of 800 g (ASTM D4060).[55] The abrader was refaced before each set of abrasion cycles using sandpaper (from Taber). Refacing was done at 25 cycles/min for 25 cycles. For abrasion, samples were abraded for up to 1,000 cycles at 60 cycles/min and a stroke length of 25.4 mm. For chemical abrasion, a Clorox wipe was attached in place of the abradant. Samples were abraded for up to 500 cycles under similar conditions. Sections (1.0 × 0.5 cm) of the mechanically abraded or Clorox wiped portions of the sample were used for bacterial testing. To test for UV stability, samples were placed 20 cm away from a 254 nm UVC mercury lamp (UVP, LLC) for 12 h at room temperature before bacterial testing. Similarly, samples were placed in a −17°C freezer for 25 h to test for low temperature stability.

Bacteria culture preparation

A single colony of bacteria from a plate previously streaked from frozen stock was grown overnight in medium. MRSA substrain COL and *P. aeruginosa* (strain ATCC

27,853) were grown in tryptic soy broth supplemented with 1% glucose (w/v, %) (TSBG) medium and *E. coli* (strain UTI89) was grown in Luria-Bertani (LB) medium at 37°C. To make the working bacteria culture for the instant kill and continuous kill experiment, 100 μL of the overnight culture was added to 2 mL of medium and allowed to grow until it reached an optical density at 600 nm (OD_{600nm}) of 0.5 OD measured with a spectrophotometer (Biochrom ULTROSPEC 2100 UV-visible spectrophotometer). For the bacteria adhesion and growth experiment, 100 μL of the overnight culture was added to 2 mL and grown to 0.5 OD_{600nm} at 37°C, and then diluted to 0.02 OD_{600nm}.

Bacteria broth culture experiment and quantification

The surfaces were cut into 1.0 cm × 0.5 cm × 1 mm sections and sterilized by UV exposure (254 nm) for 10 min on each side. Triplicate sections were used for each independent experiment. The sections were placed in 48-well plates containing 900 μL of medium and 100 μL of 0.02 OD_{600nm} bacteria culture (Figure S11 for bacteria quantification at different ODs). The 48-well plates were placed in an orbital shaking incubator (Thermo Forma) at 200 rpm and 37°C for 24 h. After incubation, the surface pieces were rinsed in 1X PBS twice, and sonicated in 2 mL of 1X PBS for 5 min to remove adhered bacteria. The PBS in the aliquot was 10-fold serially diluted by transferring 10 μL of the aliquot PBS to 90 μL of PBS in a 96-well plate. After 10-fold dilutions, 10 μL from each dilution was plated on agar and incubated for 24–48 h for viable colony enumeration. *P. aeruginosa* and MRSA were plated on tryptic soy agar (Thermo Fisher, TSA) and *E. coli* was plated on LB agar (Thermo Fisher). Then the bacteria colonies were counted and multiplied by the dilution factor to get the final number of CFUs/mL. To decrease the limit of detection (LOD) to 5 CFU/mL, 400 μL of the aliquot PBS was spread on agar in a 100 × 100 mm^2 Petri dish. As an example, adhered MRSA and *E. coli* on the surfaces of glass, polystyrene, PU, and stainless steel are shown in Figure S12.

Bacterial contact kill experiment

A modified version of ISO 22196[56] was used to test the antimicrobial performance. Sterile surfaces were cut into 1 × 1 cm squares. Surfaces were inoculated with 10 μL of working bacteria culture (~10^6 cells) and covered with a sterile 1 × 1 cm polyethylene terephthalate (PET) coverslip. Contact time was started immediately after the coverslip was placed on the surface. After the specified amount of time, the surfaces and coverslip were placed in 15 mL centrifuge tubes containing 2 mL of 1X PBS and sonicated for 5 min. This represents the recovery solution. After sonication, the aliquots were serially diluted and plated to quantify CFUs/mL.

Continuous contact kill experiment

Sterile PU and PU+35%AT surfaces were cut into 1 × 1 cm squares. Surfaces were initially inoculated with 5 μL of the working bacteria culture, and PET coverslip was placed on top. After 30 min, the surfaces and coverslips were placed in 2 mL of 1X PBS and sonicated for 5 min. For re-inoculation, another 5 μL of bacteria culture was added between the sample and new coverslip. The bacteria were enumerated 30 min after each successive re-inoculation. Up to eight re-inoculation cycles were performed. All surfaces were kept inside a covered Petri dish during the experiment.

Coating process for different applications

Keyboard

A solution of 50 mg/mL of PU+35%AT (with 0.1 wt % DBTL) was made in acetone. The solution was sprayed onto a keyboard (Hewlett-Packard) using an ATD Tools 6903 high-volume low-pressure spray gun. The coating was left to cure on the

keyboard in air, at room temperature, for 24 h. The final coating thickness was 37 ± 2 μm.

Cutting board

A solution of 2.5 g/mL of BM+35%AT (with 0.3 wt % bismuth neodecanoate catalyst) was made in acetone. The solution was brushed onto one side of the cutting board and left to cure in air, at room temperature, for 24 h.

Phone screen protector

A tempered glass screen protector was treated with O_2 plasma to remove the existing hydrophobic coating and facilitate wetting. A solution of PU+35%AT in acetone was flow coated onto the top surface of the screen protector until the excess coating material had dripped off. The final coating thickness was 200 ± 50 μm and did not impede the touch screen function of the phone (Video S2).

Medical gauze

Gauze with dimensions of 4 × 4 in (Large Microsorb Gauze Sponge; J&J) was used as the substrate choice. BM+60%AT-CMA (3:7) (with 0.3 wt % bismuth neodecanoate catalyst) was mixed without solvent. The gauze and the resin were sandwiched between aluminum foils fed through a rolling mill machine (Seattle Findings), as shown in Figure S13, until there was 0.1 g of the coating per in^2 of dressing.

Antimicrobial experiments for different applications

Keyboard

Gloved fingers were dipped in suspension of ~10^6 cells/mL of MRSA and left to dry such that a layer of MRSA coats the surface of the fingers. To mimic contamination of a keyboard during use, we typed a pangram with the MRSA-coated gloved fingers over an uncoated keyboard and a keyboard spray coated with PU+35%AT. After 10 min, contaminated keys were swabbed, and the adhered bacteria were enumerated via sonication of the swabs in 1X PBS for 5 min and serial dilution. Total swabbed area was 51 cm^2.

Cutting board

Raw pieces of chicken were allowed to thaw at room temperature for 6 h to mimic a heavy food contamination. Pieces of the thawed chicken were left to contact over the entire area of the board for 20 min. After removing the pieces, the board was left in ambient air for another 20 min followed by bacteria enumeration using swabs. Total swabbed area was 766 cm^2.

Phone screen protector

After coating the screen protector, the protector was applied to the phone. Gloved thumbs were applied with a suspension of ~10^6 cells/mL of *E. coli* (strain UTI89) and left to dry so that both thumbs had ~1.6 × 10^5 cells for each experiment. The thumbs contacted the coated and uncoated phone in a specific pattern (Figure S14) to mimic everyday use. After 2 min, the screens were swabbed for bacteria enumeration.

Medical gauze

Rectangular sections 2 × 1 cm were cut from 2-ply BM+60%AT-CMA (3:7) coated and uncoated gauze. The sections were sterilized in UV for 10 min on both sides. They were then submerged in a suspension of ~10^6 cells of *P. aeruginosa* in TSBG and left to incubate at 37°C for 24 h. After incubation, the dressings were rinsed in fresh 1X PBS for 1 min twice and submerged in aliquots containing 1X PBS for sonication and bacteria enumeration.

Skin irritation study

The skin irritation index was independently tested by NAMSA (Northwood OH), in accordance with ISO 10993-10.[57] In brief, the test involves the application of 25 × 25 mm sections of the test article to the skin of a rabbit for 23–24 h. This was followed by dermal observations at 1, 24, 48, and 72 h after removal of the test article. The degree of irritation was scored from 0 to 4. A score of 0.0 indicates no erythema and no edema observed on the skin of the animals.

SARS-CoV-2 inactivation on different surfaces

SARS-CoV-2, isolate USA-WA1/2020 (NR-52281), was obtained from BEI resources and was propagated in Vero E6 cells in DMEM supplemented with 2% FBS, 4.5 g/L D-glucose, 4 mM L-glutamine, 10 mM non-essential amino acids, 1 mM sodium pyruvate and 10 mM HEPES (DMEM-2). Infectious titers of SARS-CoV-2 were determined using median tissue culture infectious dose assay, TCID50: 10 μL drops of a 2.5 × 10^7 TCID50/mL virus stock were spotted on selected surfaces and kept for 5, 10, 30, 60, and 120 min. Virus was collected in 200 μL of PBS (after 5 min of contact time to allow full recovery of the virus). Infectious titers were determined by the TCID50 method: 25 μL of serially 10-fold diluted samples were inoculated into 96-well plates onto Vero E6 cell monolayers in septuplicate and cultured in DMEM-2. The plates were observed for cytopathic effects for 6 days. Viral titer was calculated with the Reed and Muench endpoint method.[39] TCID50-negative controls were cells incubated with medium only and included on each plate assayed. None of the negative controls had any cytopathic effect. The LOD for the TCID50 assay was determined to be 2 Log10 TCID50/mL. All experiments using SARS-CoV-2 were performed at the University of Michigan under Biosafety Level 3 (BSL3) protocols in compliance with containment procedures in laboratories approved for use by the University of Michigan Institutional Biosafety Committee and Environment, Health and Safety.

SUPPLEMENTAL INFORMATION

Supplemental information can be found online at https://doi.org/10.1016/j.matt.2022.08.018.

ACKNOWLEDGMENTS

We thank Dr. Paul Armistead, Dr. Kathy Wahl, and the Office of Naval Research for funding under grant N00014-20-1-2817. A.D. was supported by the U-M Coulter Translational Research Partnership Program, and the Rackham Predoctoral Fellowship. C.M. was supported by MICHR, grant no. UL1TR002240 and Marie-Slodovska Curie action (GA - 841247). D.B. was supported in part by NIH T-32-GM007315. J.S.V. was supported by NIH K08-AI128006 and the Taubman Institute Emerging Scholar Award. G.M. was supported by DoD W81XWH-18-1-0346. SARS-CoV-2 studies were funded by the UM Biological Sciences Scholars Program to C.E.W. We also thank James Windak in the Department of Chemistry at University of Michigan for the GC-MS test. We thank Covestro for providing raw materials for this study.

AUTHOR CONTRIBUTIONS

All authors designed the experiments, and wrote and/or edited the manuscript. A.D., T.R., and S.A.S. fabricated and tested the surfaces for bacterial studies. A.D. and Z.G. fabricated and tested the surfaces for characterization. A.D. fabricated the surfaces for virucidal studies. D.B. and C.M. tested the surfaces for virucidal

studies. C.S. tested the cytotoxicity of α-terpineol. G.M., C.E.W., J.S.V., and A.T. conceived the research.

DECLARATION OF INTERESTS

The University of Michigan has applied for a patent based on this technology. A startup company HygraTek LLC has licensed this technology from the University of Michigan. A.T. has equity and has been a paid consultant, for HygraTek LLC.

Received: March 8, 2022
Revised: July 26, 2022
Accepted: August 16, 2022
Published: August 24, 2022

REFERENCES

1. Page, K., Wilson, M., and Parkin, I.P. (2009). Antimicrobial surfaces and their potential in reducing the role of the inanimate environment in the incidence of hospital-acquired infections. J. Mater. Chem. *19*, 3819–3831. https://doi.org/10.1039/b818698g.

2. Noyce, J.O., Michels, H., and Keevil, C.W. (2006). Use of copper cast alloys to control Escherichia coli O157 cross-contamination during food processing. Appl. Environ. Microbiol. *72*, 4239–4244. https://doi.org/10.1128/AEM.02532-05.

3. Morens, D.M., Folkers, G.K., and Fauci, A.S. (2010). Erratum: the challenge of emerging and re-emerging infectious diseases (Nature (2004) 430 (242-249)). Nature *463*, 122. https://doi.org/10.1038/nature08554.

4. Dantes, R., Mu, Y., Belflower, R., Aragon, D., Dumyati, G., Harrison, L.H., Lessa, F.C., Lynfield, R., Nadle, J., Petit, S., et al. (2013). National burden of invasive methicillin-resistant Staphylococcus aureus infections, United States, 2011. JAMA Intern. Med. *173*, 1970–1978. https://doi.org/10.1001/jamainternmed.2013.10423.

5. Otter, J.A., Yezli, S., and French, G.L. (2011). The role played by contaminated surfaces in the transmission of nosocomial pathogens. Infect. Control Hosp. Epidemiol. *32*, 687–699. https://doi.org/10.1086/660363.

6. Dancer, S.J. (2014). Controlling hospital-acquired infection: focus on the role of the environment and new technologies for decontamination. Clin. Microbiol. Rev. *27*, 665–690. https://doi.org/10.1128/CMR.00020-14.

7. Kramer, A., Schwebke, I., and Kampf, G. (2006). How long do nosocomial pathogens persist on inanimate surfaces? A systematic review. BMC Infect. Dis. *6*, 130–138. https://doi.org/10.1186/1471-2334-6-130.

8. Lawrence, C.A., and Block, S.S. (2000). Disinfection, Sterlization, and Preservation (Lippincott Williams & Wilkins).

9. Mazzola, P.G., Penna, T.C.V., and Martins, A.M.D.S. (2003). Determination of decimal reduction time (D value) of chemical agents used in hospitals for disinfection purposes. BMC Infect. Dis. *3*, 24. https://doi.org/10.1186/1471-2334-3-24.

10. Rutala, W.A., and Weber, D.J.; Healthcare Infection Control Practices Advisory, C. (2008). Guideline for disinfection and sterilization in healthcare facilities, 2008. http://www.cdc.gov/hicpac/Disinfection_Sterilization/10_0MiscAgents.html.

11. Hans, M., Erbe, A., Mathews, S., Chen, Y., Solioz, M., and Mücklich, F. (2013). Role of copper oxides in contact killing of bacteria. Langmuir *29*, 16160–16166. https://doi.org/10.1021/la404091z.

12. Molteni, C., Abicht, H.K., and Solioz, M. (2010). Killing of bacteria by copper surfaces involves dissolved copper. Appl. Environ. Microbiol. *76*, 4099–4101. https://doi.org/10.1128/AEM.00424-10.

13. Wilks, S.A., Michels, H., and Keevil, C.W. (2005). The survival of Escherichia coli O157 on a range of metal surfaces. Int. J. Food Microbiol. *105*, 445–454. https://doi.org/10.1016/j.ijfoodmicro.2005.04.021.

14. Grass, G., Rensing, C., and Solioz, M. (2011). Metallic copper as an antimicrobial surface. Appl. Environ. Microbiol. *77*, 1541–1547. https://doi.org/10.1128/AEM.02766-10.

15. Agnihotri, S., Mukherji, S., and Mukherji, S. (2013). Immobilized silver nanoparticles enhance contact killing and show highest efficacy: elucidation of the mechanism of bactericidal action of silver. Nanoscale *5*, 7328–7340. https://doi.org/10.1039/c3nr00024a.

16. Lemire, J.A., Harrison, J.J., and Turner, R.J. (2013). Antimicrobial activity of metals: mechanisms, molecular targets and applications. Nat. Rev. Microbiol. *11*, 371–384. https://doi.org/10.1038/nrmicro3028.

17. Severin, B.F., Suidan, M.T., and Engelbrecht, R.S. (1983). Kinetic modeling of U.V. disinfection of water. Water Res. *17*, 1669–1678. https://doi.org/10.1016/0043-1354(83)90027-1.

18. Mahmoud, B.S.M., and Linton, R.H. (2008). Inactivation kinetics of inoculated Escherichia coli O157:H7 and Salmonella enterica on lettuce by chlorine dioxide gas. Food Microbiol. *25*, 244–252. https://doi.org/10.1016/j.fm.2007.10.015.

19. Jung, W.K., Koo, H.C., Kim, K.W., Shin, S., Kim, S.H., and Park, Y.H. (2008). Antibacterial activity and mechanism of action of the silver ion in Staphylococcus aureus and Escherichia coli. Appl. Environ. Microbiol. *74*, 2171–2178. https://doi.org/10.1128/AEM.02001-07.

20. Zhao, G., and Stevens, S.E. (1998). Multiple parameters for the comprehensive evaluation of the susceptibility of Escherichia coli to the silver ion. Biometals *11*, 27–32. https://doi.org/10.1023/A:1009253223055.

21. Matsumura, Y., Yoshikata, K., Kunisaki, S.i., and Tsuchido, T. (2003). Mode of bactericidal action of silver zeolite and its comparison with that of silver nitrate. Appl. Environ. Microbiol. *69*, 4278–4281. https://doi.org/10.1128/AEM.69.7.4278-4281.2003.

22. Delgado, K., Quijada, R., Palma, R., and Palza, H. (2011). Polypropylene with embedded copper metal or copper oxide nanoparticles as a novel plastic antimicrobial agent. Lett. Appl. Microbiol. *53*, 50–54. https://doi.org/10.1111/j.1472-765X.2011.03069.x.

23. Pichersky, E., and Gang, D.R. (2000). Genetics and biochemistry of secondary metabolites in plants: an evolutionary perspective. Trends Plant Sci. *5*, 439–445. https://doi.org/10.1016/S1360-1385(00)01741-6.

24. Wagner, G.J. (1991). Secreting glandular trichomes: more than just hairs. Plant Physiol. *96*, 675–679. https://doi.org/10.1104/pp.96.3.675.

25. Burt, S. (2004). Essential oils: their antibacterial properties and potential applications in foods - a review. Int. J. Food Microbiol. *94*, 223–253. https://doi.org/10.1016/j.ijfoodmicro.2004.03.022.

26. Davidson, P.M. (1997). Chemical preservatives and natural antimicrobial compounds. In Food Microbiology: Fundamentals and Frontiers, M.P. Doyle, L.R. Beuchat, and T.J. Montville, eds. (ASM), pp. 520–556.

27. Denyer, S.P., and Stewart, G.S.A.B. (1998). Mechanisms of action of disinfectants. Int. Biodeterior. Biodegrad. *41*, 261–268. https://doi.org/10.1016/S0964-8305(98)00023-7.

28. Sikkema, J., de Bont, J.A., and Poolman, B. (1995). Mechanisms of membrane toxicity of hydrocarbons. Microbiol. Rev. *59*, 201–222. https://doi.org/10.1128/Mmbr.59.2.201-222.1995.

29. Bauer, K., Garbe, D., and Surburg, H. (1997). Common Fragrance and Flavor Materials: Preparation, Properties and Uses, 3rd Edition (Wiley-VCH).

30. Carson, C.F., Hammer, K.A., and Riley, T.V. (2006). Melaleuca alternifolia (Tea Tree) oil: a review of antimicrobial and other medicinal properties. Clin. Microbiol. Rev. *19*, 50–62. https://doi.org/10.1128/CMR.19.1.50-62.2006.

31. C. F. R. § 172.515. (2022). In F.a.D. Administration, ed. https://www.accessdata.fda.gov/scripts/cdrh/cfdocs/cfcfr/CFRSearch.cfm?FR=172.515.

32. Commission Implementing Regulation (EU) No 872/2012 of 1 October 2012 adopting the list of flavouring substances provided for by Regulation (EC) No 2232/96 of the European Parliament and of the Council, introducing it in Annex I to Regulation (EC) No 1334/2008 of the European Parliament and of the Council and repealing Commission Regulation (EC) No 1565/2000 and Commission Decision 1999/217/EC. In E. Commission, ed. Publications Office of the EU.

33. Langer, R., and Folkman, J. (1976). Polymers for the sustained release of proteins and other macromolecules. Nature *263*, 797–800.

34. Ekladious, I., Colson, Y.L., and Grinstaff, M.W. (2019). Polymer–drug conjugate therapeutics: advances, insights and prospects. Nat. Rev. Drug Discov. *18*, 273–294. https://doi.org/10.1038/s41573-018-0005-0.

35. Golovin, K., and Tuteja, A. (2017). A predictive framework for the design and fabrication of icephobic polymers. Sci. Adv. *3*, e1701617-9. https://doi.org/10.1126/sciadv.1701617.

36. Krawczyk, J., Croce, S., McLeish, T.C.B., and Chakrabarti, B. (2016). Elasticity dominated surface segregation of small molecules in polymer mixtures. Phys. Rev. Lett. *116*, 208301. https://doi.org/10.1103/PhysRevLett.116.208301.

37. Bico, J., Thiele, U., and Quéré, D. (2002). Wetting of textured surfaces. Colloids Surf. A Physicochem. Eng. Asp. *206*, 41–46. https://doi.org/10.1016/S0927-7757(02)00061-4.

38. de Gennes, P.-G., Brochard-Wyart, F., and Quéré, D. (2004). Capillarity and Wetting Phenomena: Drops, Bubbles, Pearls, Waves. https://doi.org/10.1007/978-0-387-21656-0_9.

39. Reed, L.J., and Muench, H. (1938). A simple method of estimating fifty per cent endpoints. Am. J. Epidemiol. *27*, 493–497. https://doi.org/10.7723/antiochreview.72.3.0546.

40. Chick, H. (1908). An investigation of the laws of disinfection. J. Hyg. *8*, 92–158. https://doi.org/10.1017/S0022172400006987.

41. Lambert, R.J., and Johnston, M.D. (2000). Disinfection kinetics: a new hypothesis and model for the tailing of log-survivor/time curves. J. Appl. Microbiol. *88*, 907–913. https://doi.org/10.1046/j.1365-2672.2000.01060.x.

42. Doremalen, V. (2020). Aerosol and surface stability of SARS-CoV-2 as compared with SARS-CoV-1. N. Engl. J. Med. *382*, 1564–1567.

43. Vincent, J.-L., Rello, J., Marshall, J., Silva, E., Anzueto, A., Martin, C.D., Moreno, R., Lipman, J., Gomersall, C., Sakr, Y., and Reinhart, K.; EPIC II Group of Investigators (2009). International study of the prevalence and outcomes of infection in intensive care units. JAMA *302*, 2323–2329.

44. Baym, M., Stone, L.K., and Kishony, R. (2016). Multidrug evolutionary strategies to reverse antibiotic resistance. Science *351*. aad3292:1–8. https://doi.org/10.1126/science.aad3292.

45. Gross, T.M., Lahiri, J., Golas, A., Luo, J., Verrier, F., Kurzejewski, J.L., Baker, D.E., Wang, J., Novak, P.F., and Snyder, M.J. (2019). Copper-containing glass ceramic with high antimicrobial efficacy. Nat. Commun. *10*, 1979–1988. https://doi.org/10.1038/s41467-019-09946-9.

46. Weber, D.J., and Rutala, W.A. (2013). Self-disinfecting surfaces: review of current methodologies and future prospects. Am. J. Infect. Control *41*, S31–S35. https://doi.org/10.1016/j.ajic.2012.12.005.

47. Chin, A.W.H., Poon, L.L.M., Perera, M.R.A., Hui, K.P.Y., Yen, H.-L., Chan, M.C.W., Peiris, M., and Poon, L.L.M. (2020). Stability of SARS-CoV-2 in different environmental conditions. Lancet. Microbe *1*, e146. https://doi.org/10.1016/S2666-5247(20)30003-3.

48. Hosseini, M., Behzadinasab, S., Benmamoun, Z., and Ducker, W.A. (2021). The viability of SARS-CoV-2 on solid surfaces. Curr. Opin. Colloid Interface Sci. *55*, 101481. https://doi.org/10.1016/j.cocis.2021.101481.

49. Kraay, A.N.M., Hayashi, M.A.L., Berendes, D.M., Sobolik, J.S., Leon, J.S., and Lopman, B.A. (2021). Risk for fomite-mediated transmission of SARS-CoV-2 in child daycares, schools, nursing homes, and offices. Emerg. Infect. Dis. *27*, 1229–1231. https://doi.org/10.3201/eid2704.203631.

50. Cohen, M.L. (1992). Epidemiology of drug resistance: implications for a post-antimicrobial era. Science *257*, 1050–1055. https://doi.org/10.1126/science.257.5073.1050.

51. Baker-Austin, C., Wright, M.S., Stepanauskas, R., and McArthur, J.V. (2006). Co-selection of antibiotic and metal resistance. Trends Microbiol. *14*, 176–182. https://doi.org/10.1016/j.tim.2006.02.006.

52. Bruins, M.R., Kapil, S., and Oehme, F.W. (2000). Microbial resistance to metals in the environment. Ecotoxicol. Environ. Saf. *45*, 198–207. https://doi.org/10.1006/eesa.1999.1860.

53. Wiegand, I., Hilpert, K., and Hancock, R.E.W. (2008). Agar and broth dilution methods to determine the minimal inhibitory concentration (MIC) of antimicrobial substances. Nat. Protoc. *3*, 163–175. https://doi.org/10.1038/nprot.2007.521.

54. Hammer, K.A., Carson, C.F., and Riley, T.V. (2012). Effects of Melaleuca alternifolia (tea tree) essential oil and the major monoterpene component terpinen-4-ol on the development of single- and multistep antibiotic resistance and antimicrobial susceptibility. Antimicrob. Agents Chemother. *56*, 909–915. https://doi.org/10.1128/AAC.05741-11.

55. ASTM D4060-19 Standard test method for abrasion resistance of organic coatings by the taber abraser, ASTM International, West Conshohocken, PA, 2019. https://doi.org/10.1520/D4060-19.

56. International Organization for Standards (2011). ISO 22196: Measurement of antibacterial activity on plastics and other non-porous surfaces. Retrieved from https://www.iso.org/standard/54431.html.

57. International Organization for Standards (2011). ISO 10993-10: Biological evaluation of medical devices - part 10: Tests for irritation and skin sensitization. Retrieved from https://www.iso.org/standard/40884.html